J Mater Sci (2007) 42:4461–4469
DOI 10.1007/s10853-006-0412-1

Synthesis of 3-dimensional mesoporous silica using a di-block copolymer template

Jinlan Ju · Huining Xiao · Zisheng Zhang

Received: 20 January 2006 / Accepted: 5 May 2006 / Published online: 14 February 2007

Abstract Exploring polymeric surfactants as templates for synthesizing ordered mesoporous silicas has become increasingly important for both academic interests and industrial applications. In this work, we employed $C_{16}EO_{40}$, a di-block copolymer polyethylene-poly(ethylene oxide), as template in an attempt to synthesize a modified 3-dimensional wormhole mesoporous silicas (WMS-39). In addition, various synthesizing conditions were investigated, including pre-hydrolysis time of TEOS, reaction temperatures and the ratios of TEOS to template. The products were characterized using powder XRD, TEM, ^{29}Si MAS NMR and nitrogen adsorption measurements. The characteristics of as-synthesized mesoporous silica were compared with SBA-15, a highly ordered mesoporous silica, prepared using non-ionic tri-block copolymers of poly(ethylene oxide)–poly(propylene oxide)–poly(ethylene oxide) as templates. The WMS-39 materials have a BET surface area of 600–970 m^2/g and narrowly distributed pore diameter around 3.9 nm. The morphology of WMS-39 was found to be wormhole framework as indicated in TEM diagrams. Thermal transformation of the as-synthesized mesoporous materials were carefully analyzed with TGA/DTA. Findings obtained from this work enable us to propose a modified assembly mechanism of mesoporous silicas.

Introduction

Mesoporous material MCM-41 (Mobile Crystalline Material), developed by Mobile researchers more than a decade ago, is a silicate with a hexagonal ordered pore structure and a narrow pore size distribution. The success in synthesizing MCM-41 has sparked the interest in studying mesoporous materials [1, 2]. Due to their high surface areas and uniform pore diameters in the range of 2–50 nm, the mesoporous materials have great potential to be utilized as catalyst supports, especially suitable for the reactions involving bulky molecules which are difficult to diffuse into and out of conventional microporous catalyst supports. HMS is referred to hexagonal mesoporous silica (HMS), which is less ordered and shows a wormhole-like pore structure.

MCM-41 has been applied to deep-hydrodesulfurization of light cycle oil (LCO) as catalyst supports [3–5] while HMS was prepared and used as photocatalyst supports [6–8]. In addition, SBA-15 has been intensively investigated because of its ordered and monodispersed hexagonal mesopores together with its thicker walls [9–15]. Trong et al. reviewed the potential applications of these three meso-structured materials (i.e., MCM-41, HMS and SBA-15) in catalysis and indicated that HMS with wormhole framework allowed a faster diffusion of reactants than MCM-41

J. Ju · H. Xiao (✉)
Department of Chemical Engineering, University of New Brunswick, Fredericton, NB, CanadaE3B 5A3
e-mail: hxiao@unb.ca

Z. Zhang
Department of Chemical Engineering, University of Ottawa, Ottawa, ON, CanadaK1N 6N5

H. Xiao
State Key Lab of Pulp & Paper Eng., South China University of Technology, Guangzhou, China

and SBA-15 [16]. The tunnels (or connections) among the mesopores of HMS are shortened to enable reactants and products diffuse faster, which is an important property for catalyst supports.

SBA-15 can be synthesized using an amphiphic triblock copolymer [poly(ethylene oxide)–poly(propylene oxide)–poly(ethylene oxide), EO-PO-EO] as an organic structure-directing agent under acidic condition. Stucky et al. proposed the self-assembly mechanism of SBA-15 [10–14]. More recently, non-ionic alkyl poly(ethylene oxide) (C_xEO_y) oligomers were employed as templates to synthesize mesoporous silicas following the same assembly mechanism as SBA-15. Cubic mesoporous silica (SBA-11) with *Pm3m* diffraction symmetry was synthesized in the presence of Brij56 ($C_{16}EO_{10}$) surfactant, while a 3-d hexagonal (*P63/mmc*) mesoporous silica structure (SBA-12) was obtained when Brij76 ($C_{18}EO_{10}$) was used. Due to the short molecular chains, the average pore sizes of SBA-11 and SBA-12 were only about 2.5 and 3.1 nm, respectively. It can be concluded that the slight difference on the length of hydrophobic segment between Brij76 and Brij56 leads to a great diversity of the mesoporous structures though the same assembly mechanism were followed. Smarsly et al. [17] carefully investigated the dependence of the porosity on the block lengths or the block volume of C_xEO_y oligomers up to $C_{12}EO_{30}$.

In this work, a longer di-block copolymer PE/PEO resin ($C_{16}EO_{40}$) was applied as the template to synthesize larger mesoporous silicas. The number of hydrophilic ethylene oxide (EO) repeat units is 40, much higher than that of Brij56 and Brij76. It has been reported that the relatively long hydrophilic EO blocks of the copolymer as templates tend to form large mesopores with relatively thick silica wall [18, 19]. In addition, the shape of micelles depends on the size of either hydrophilic head or hydrophobic tail of a surfactant [20]. Therefore, though the repeat units of the PE/EO template are the same as the Brij surfactants, their micelle structures in water could be significantly different and consequently result in different mesoporous silicas.

As mentioned above, molecules diffuse faster in the catalyst supports with wormhole mesoporous framework than those with long cylindrical tunnels. Our key objective was to synthesize a 3-dimensional wormhole silica with narrowly distributed pore size using the PE/PEO surfactant as template and tetraethyl orthosilicate (TEOS) as silica source. Another important aspect is that the pre-hydrolysis of TEOS influences on the characteristics of the resulting mesoporous silica. Because the solubilization of TEOS into micelles is much faster than the hydrolysis, it is necessary to hydrolyze TEOS prior to adding it to the template solution. The products were well-characterized using powder XRD, N_2 Adsorption/desorption measurement, TEM and ^{29}Si MAS NMR. The comparison between the synthesized mesoporous silica and SBA-15 was also made since both of them were prepared using block polymers as templates.

Experimental

Materials

The di-block polymer template PE/PEO, Pluronic P123 and tetraethylorthosilicate (TEOS) were used as received from Aldrich. The PE/PEO (Mn = 2,250) contained 80 wt% hydropholic ethylene oxide segment. The Pluronic P123 (Mn = 5,800) is a tri-block copolymer ($EO_{20}PO_{70}EO_{20}$). Aqueous HCl acid (37%) was obtained from Fluka.

Syntheses of mesoporous silicas

The 3-dimensional wormhole mesoporous materials (WMS-39) were synthesized in an acid medium under hydrothermal conditions, using TEOS as a silica precursor and PE/PEO as a structure-directing agent. In a typical preparation, a certain amount of PE/PEO (based on the weight ratio of template/TEOS) was dissolved in an aqueous HCl solution with vigorous stirring to form a template solution. Silica source tetraethyl orthosilicate (TEOS) was pre-hydrolyzed in a 2 M HCl aqueous solution at the mole ratio of water/TEOS of 16. The solution was vigorously stirred at ambient for 0.5–3 h to obtain a solution which was then dropped to the template solution. The mixture was first allowed to react at 40 °C for 24 h and then to age at 80 °C for another 2 days. The solid product was recovered, washed and dried at 100 °C to obtain the as-synthesized product, a kind of nanocomposite of polymer/silica. The as-synthesized samples were calcinated by slowly increasing the temperature from room temperature to 550 °C and maintained at 550 °C for 20 h to produce the final 3-dimensional wormhole mesoporous silica (WMS-39). The yield was calculated via dividing the weight of solid product after calcinations by the theoretical weight of SiO_2.

SBA-15 was synthesized following the procedure reported by Zhao et al. using a Pluronic P123 tri-block copolymer ($EO_{20}PO_{70}EO_{20}$) as a template [9–11]. 1.92 g Pluronic P123 was dissolved in 15 g water and

120 g of 2 M HCl solution at 35 °C. Then 4 g TEOS was added into the homogeneous template solution with stirring 35 °C for 24 h. The resulting mixture was aged at 80 °C for 24 h without stirring. The solid product was recovered, washed, and dried at 100 °C. Calcination was carried out at the same conditions as described above.

Characterizations

Powder X-ray diffraction (XRD) patterns were taken on a Bruker AXS D8 ADVANCE diffractometer equipped with a liquid nitrogen cooled germanium solid-state detector using CuK_α radiation.

Nitrogen adsorption/desorption isotherms at 77 K were established using a Quantachrome Autosorb automated gas sorption system. The sample was pretreated at 200 °C overnight in the vacuum line. The BET surface area was determined from the linear part of the BET equation. The mesopore size distribution was determined from the desorption branch of the N_2 adsorption/desorption isotherms using the Barrett–Joyner–Halenda (BJH) formula. The pore volume was taken at the $P/P_0 = 0.985$ single point.

High-resolution solid-state ^{29}Si MAS NMR spectra were recorded on a Chemagnetics CMX-500 spectrometer operating at a ^{29}Si resonance frequency of 79.50 MHz under the conditions of magic-angle spinning at 3 kHz at room temperature; $\pi/2$ pulse lengths of 6–7 μs were used to acquire one-pulse ^{29}Si spectra are referenced to tetramethlysilane, $Si(CH_3)_4$.

Transmission electron micrographs (TEM) were taken on a JEOL 2010 electron microscope operating at 200 keV. The samples for TEM were prepared by dispersing a large amount of slurry in ethanol onto a cupper grid coated with carbon.

A Du Pont TGA51 Themogravimetric Analyzer coupled with 910 Differential Scanning Calorimeter was used for simultaneous thermal analysis combining thermogravimetry (TG), derivate thermogravity (DTG), and difference thermoanalysis (DTA) from ambient to 1,173 K with a heating rate of 5 K min^{-1} under nitrogen flow.

Results and discussion

Pre-hydrolysis of TEOS

TEOS can undergo the hydrolysis catalyzed by HCl acid to form protonated silicic acid $[Si(OH)_4]$ (I^+) at pH less than 2, which is the isoelectric point of the silicic acid. The protonated silicic acid then condensation-polymerizes to form silica network [9, 21], as shown in Scheme 1. The time interval between hydrolysis and condensation is dependent on the mole ratio of water to TEOS (*W*) [21]. Higher *W* values (*W* = 10) enhance hydrolyzing rates and thereby make hydrolysis nearly complete prior to condensation under acid conditions. During the hydrolysis and condensation process, protonated silicic acid can be directed by anionic, neutral or non-ionic templates to form various silicas with desired structures.

In this work, the syntheses were performed at different acidities employing the di-block copolymer surfactant PE/PEO as the templates. Results are shown in Table 1. It was found that if TEOS was directly dropped into the template solution, no precipitation

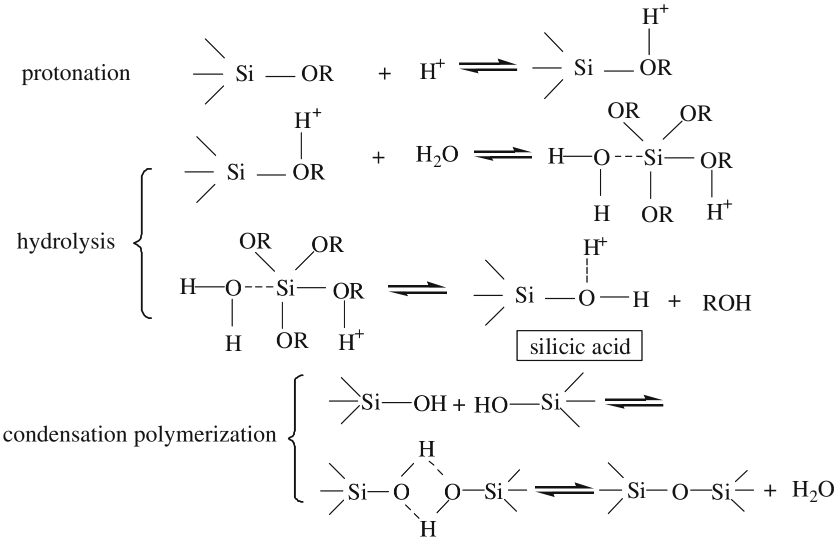

Scheme 1 TEOS hydrolysis and condensation polymerization at acid conditions

Table 1 The influence of template content on yield

Weight ratio of template/TEOS (w/w)	HCl concentration (M)		
	0.8	1.6	2
	Yield[a] (%)		
0.125	82.3	91.9	80.2
0.188	74.6	87.2	65.4
0.25	62.9	Nppt	Nppt
0.5	Nppt[b]	Nppt	Nppt
0.75	Nppt	Nppt	Nppt
1	Nppt	Nppt	Nppt

[a] The yield was evaluated after calcinating product

[b] Nppt, no precipitation; TEOS was directly added into template solutions

occurred at the weight ratio of template/TEOS higher than 0.5 even after the samples have been hydrothermally treated for 2 days. When the weight ratio of template/TEOS was reduced to 0.25, the precipitation occurred. The noticeable amount of white solid products was obtained at the ratio of 0.19. However, if TEOS was first allowed to pre-hydrolyze in HCl solution prior to being added into the template solutions, precipitation always appeared and the yield was higher than 95% even the ratio of template/TEOS was as high as 0.75 (see Table 2).

Figure 1 shows the yield as a function of the pre-hydrolysis time of TEOS. There were three clear steps for the pre-hydrolysis of TEOS. It took 20 min for the undissolvable TEOS to gradually hydrolyze to the $Si(OH)_4$ miscible with HCl solution and finally a clear solution was obtained. Then the solution turned to turbid but no precipitation because of the less condensation of silicic acid, similar to that reported by Pouxviel et al. [22] After TEOS had been hydrolyzed for 200 min, some solid was observed in the turbid solution due to the polycondensizing of silicic acid. Obviously, it is impossible for the PE/PEO template further direct the solid silica polymer to build the expecting mesoporous structure. Thus we did not synthesize mesoporous silicas using the TEOS pre-hydrolyzed for longer than 200 min. As indicated in Fig. 1, no products could be obtained if the pre-hydrolysis time of TEOS was less than 60 min, whereupon the yield enhanced fast with increasing the pre-hydrolysis time of TEOS and achieved the highest yield when TEOS had pre-hydrolyzed for 150 min.

Table 2 Yields at different contents of template

Weight ratio of template/TEOS (w/w)	HCl concentration (M)	
	1.6	2
	Yield[*]	
0.125	93.5	87.6
0.188	100	90.1
0.25	96.3	82.4
0.5	97.5	76.0
0.75	94.5	83.3
1	72.7	66.4

[*] TEOS was pre-hydrolyzed for 180 min

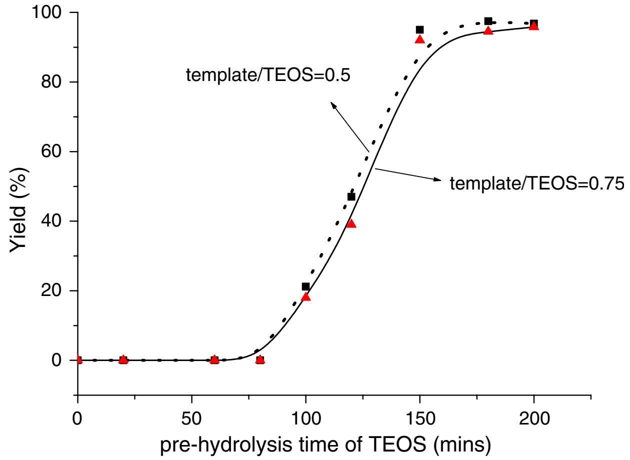

Fig. 1 Yield as a function of pre-hydrolysis time of TEOS. [HCl] = 1.6 M

XRD

The powder X-ray diffraction patterns were measured for both as-synthesized and calcinated WMS-39s. Since the pre-hydrolysis time of TEOS is a key factor for the preparation of WMS-39, it is necessary to record how the XRD patterns of the calcinated samples vary with the pre-hydrolysis time. As seen from Fig. 2, all XRD

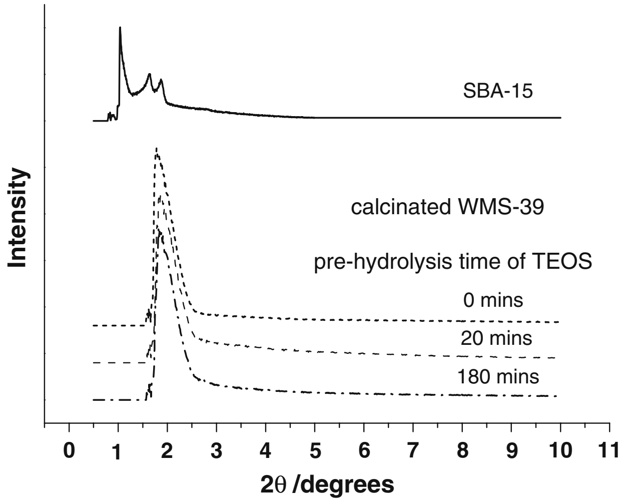

Fig. 2 XRD of calcinated samples experienced different pre-hydrolysis time of TEOS. The ratio of template/TEOS is 0.19

patterns for WMS-39s are different from that of the hexagonal SBA-15, and exhibit a single diffraction peak at 2θ around 2° corresponding to d_{100} spacing about 4 nm. However, the patterns are independent on the pre-hydrolysis time of TEOS. Higher ordered Bragg reflections of the hexagonal structure are not resolved. The XRD patterns are similar to that of HMS [6], implying the wormhole structure of WMS-39s. The similar patterns were observed for all as-synthesized samples as well.

Nitrogen adsorption/desorption isotherm

Important trends are revealed by the N_2 adsorption/desorption isotherms in Fig. 3; and the corresponding BJH pore size distribution curves are shown in Fig. 4. The isotherms feature hysteresis loops with a steep inflection around P/P_0 = 0.4–0.5 indicating that the pores are in the mesoporous region [22–24]. The pre-hydrolysis time of TEOS again plays such an important role that the hysteresis loop shift to higher volume with increasing the pre-hydrolysis time of TEOS. Both the pore volume and BET surface area increase correspondingly to prolonging the pre-hydrolysis time and achieve the maximum when the pre-hydrolysis time is 150 min, as indicated in Fig. 5. However, the plot of BJH pore diameter distribution shows that the narrow distributed pore diameters are independent of the pre-hydrolysis time of TEOS, which again reflects that the pore diameters are controlled by the micelle size instead of the silica source.

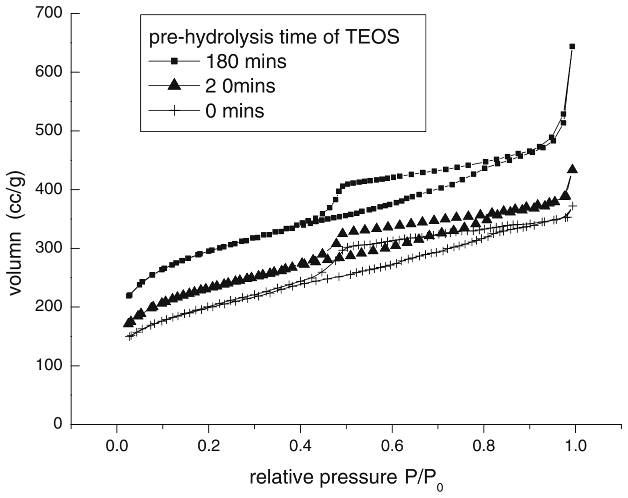

Fig. 3 N_2 adsorption/desorption isotherms for calcinated samples synthesized at various pre-hydrolysis time of TEOS

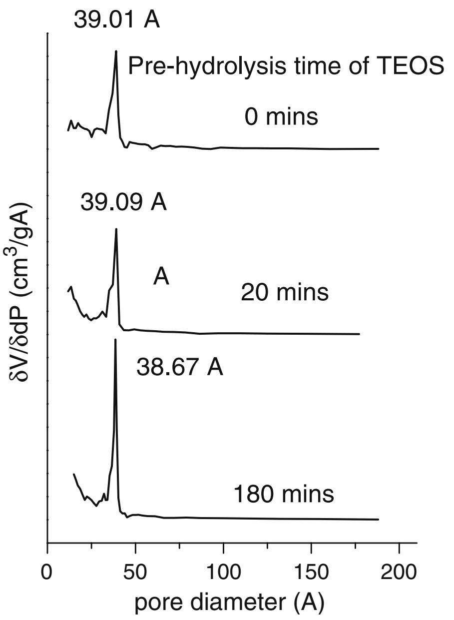

Fig. 4 BJH mesoporous diameter distribution for samples synthesized at various pre-hydrolysis times of TEOS

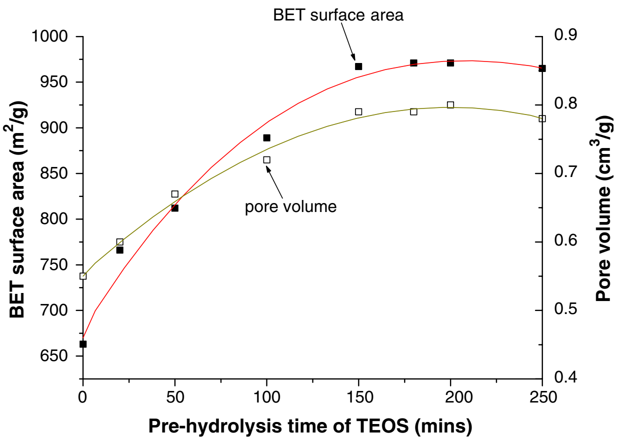

Fig. 5 Both pore volume and BET surface area as functions of pre-hydrolysis time of TEOS for the samples prepared at the ratio of template/TEOS = 0.19

TEM

The WMS-39, the mesoporous silica prepared using PE/PEO template possesses a uniform pore size and a disordered wormhole-like meso-structure, which is further confirmed with TEM, as shown in Fig. 6A. Both the pore diameter and wall thickness are even for WMS-39. In contrast, the pore structure of SBA-15 is ordered hexagonal (see Fig. 6B), which was synthesized under the conditions similar to those for WMS-39. The difference between WMS-39 and SBA-15 might result from the different micelle structures formed by the di-block copolymer and tri-block

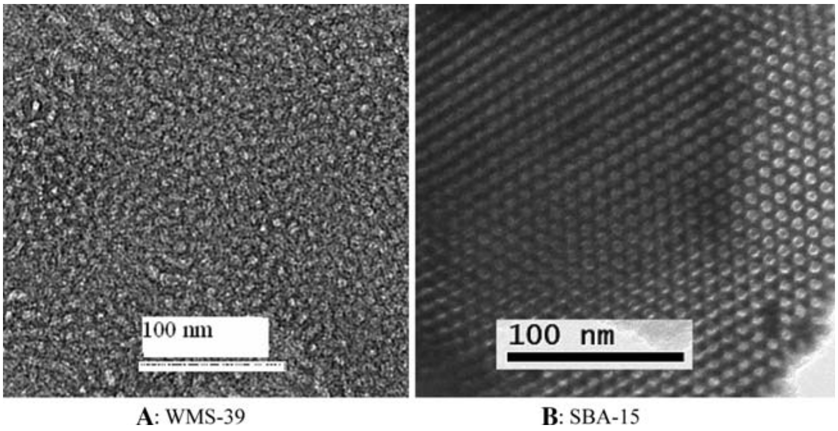

A: WMS-39 **B**: SBA-15

Fig. 6 TEM images of the calcinated WMS-39 and SBA-15

copolymer, respectively. In addition, the particle size of WMS-39 is much smaller than that of SBA-15, as indicated in Fig. 7.

Silicon environments and solid-state NMR spectroscopy

Magic-angle spinning (MAS) makes it possible in solid-state NMR spectroscopy to obtain high-resolution ^{29}Si spectra. This technique averages the chemical shift anisotropy and dipolar interactions that otherwise would cause very broad lines. Through siloxane bonds, a silicon atom can be bonded to a maximum of four other silicon nuclei [25, 26], as shown in Fig. 8. If a ^{29}Si nucleus is bonded to four other silicon atoms, the chemical shift of this so-called Q^4 species lies around –110 ppm. For every siloxane bond less, a shift of about 10 ppm occurs. Therefore, Q^2 has a chemical shift around –110 + 2*10 = –90 ppm.

Figure 9 shows the ^{29}Si MAS NMR spectra for the calcinated SBA-15, as-synthesized WMS-39 and calcinated WMS-39 aged at 80 °C for 48 h. In SBA-15, the broad peak at 111 ppm in the NMR spectrum of SBA-15 indicates that most of silicon atoms are bonded with

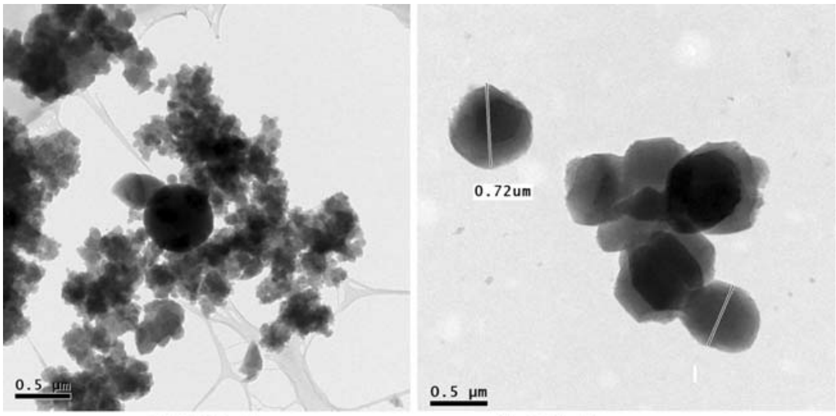

A: WMS-39 **B**: SBA-15

Fig. 7 TEM images of the particles of calcinated WSM-39 and SBA-15

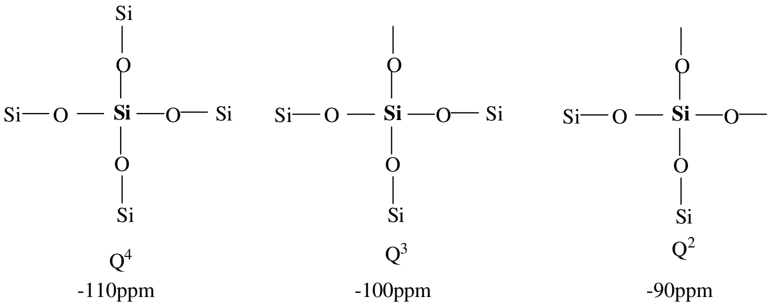

Fig. 8 Effect of silicon environments on chemical shifts. Groups not depicted are alkoxy or silanol

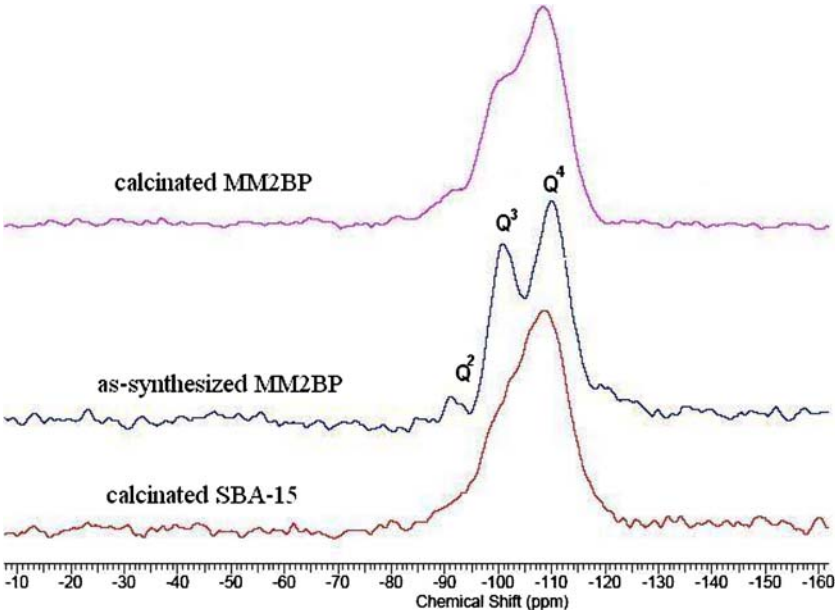

Fig. 9 Comparison of ^{29}Si MAS NMR spectra of WMS-39 and calcinated SBA-15

other four silicon atoms. However, the status of silicon in WMS-39 is complicated. The as-synthesized WMS-39 exhibits two main broad resonances at –111, –102 ppm, and a very weak resonance at –92 ppm assigned to Q^4, Q^3, and Q^2, respectively. After calcination at 550 °C for 10 h, the ^{29}Si MAS NMR spectrum shows a sharp (Q^4) resonance at –111 ppm and a decrease in the (Q^3) resonance at –102 and –92 ppm, suggesting that the calcinations facilitates further condensation reaction of the silanol groups in the silica matrix and improve hydrophobicity of the samples simultaneously.

TGA

TGA and DTA of the as-synthesized WMS-39 materials were performed in nitrogen gas at a heating rate of 5 °C/min. The TGA curves in Fig. 10 show three stages of weight loss, attributed primarily to: (I) desorption of molecular water, (II) decomposition and desorption of organic templates, and (III) water desorption via condensation of silanol groups resulting in the formation of siloxane bonds [27]. The temperature ranges for the each stage of weight loss vary with the pre-hydrolysis time of TEOS. The overall weight losses were 40.5 and 34.5% for the sample prepared using the TEOS which had been pre-hydrolyzed for 180 min (sample A) and 20 min (sample B), respectively. It is interesting that under nitrogen atmosphere, the decomposition of the polymeric template took place at relatively high temperatures (the maximum on the weight loss occurred at about 650 °C). This is similar to the template behave for SBA-15 as reported by Kruk et al. [27].

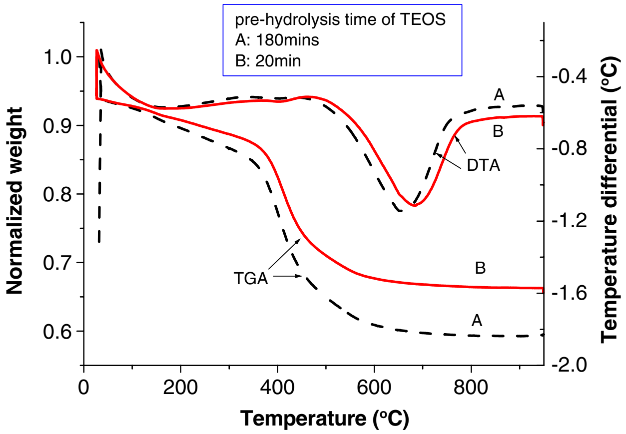

Fig. 10 TGA and DTA patterns for as-synthesized WMS-39 materials obtained from using different pre-hydrolysis time of TEOS

The high decomposition temperature of the template under nitrogen atmosphere is in contrast to the decomposition under air atmosphere, where most of the template was removed below 500 °C [8]. It is worthy to note that a endothermic peak at 650 °C for sample A and 685 °C for sample B on the DTA curves were observed, indicating water desorption as condensation of silanol groups along with the transformation of mesoporous structure.

Formation process of mesoporous silicate

In a strong acidic aqueous solution, amphiphilic polymers containing poly(ethylene oxide) segments can be solvated by hydronium ions H_3O^+ via hydrogen-bond to form S^0H^+ species [28]. When the template is dissolved in aqueous HCl solution at its concentration higher than the critical micelle concentration (CMC), the PE/PEO micelles are formed with hydrophilic ethylene oxide shell exposing to water and the hydrophobic polyethylene as core. The oxygen rich head EO fragments are solvated by hydronium ions H_3O^+ from solution via hydrogen bond and further are neutralized by Cl^- ions from the solution to form charged cluster $S^0H^+Cl^-$.

The $S^0H^+Cl^-$ cluster attracts the protonated silicic acid (I^+) to produce the assembly species of $S^0H^+Cl^-I^+$ and provides the interface of the cooperative organization of the polymer and inorganic species. Inorganic TEOS hydrolyzes, condensation-polymerizes on the surface of the template micelles to generate the final mesoporous materials WMS-39. Due to the amphiphilic properties of PE/PEO, TEOS can fast diffuse into the PE/PEO micelle core, resulting in the isolation of TEOS from HCl acid and preventing from being hydrolyzed. If the ratio of template/TEOS is higher than 0.25, all TEOS would be encapsulated in PE/PEO shell and only a homogeneous polymer/TEOS/HCl/H_2O solution would be gained. If the ratio of template/TEOS were lower than 0.25, there would be no sufficient micelles in the solution to capsulate TEOS and TEOS could undergo hydrolysis to form silica. To avoid TEOS being encapsulated in the micelles, TEOS was first allowed to be hydrolyzed in HCl aqueous solution to form protonated silicic acid and then dropped into the template solution. The hydrophilic protonated silicic acid could condensation-polymerize to form continuous silica wall around the templates, leading to the wormhole structure.

Conclusions

A modified 3-dimensional mesoporous silica (WMS-39) was synthesized by a sol–gel approach in a strong acidic aqueous media using a non-ionic poly(ethlylene)-b-poly(ethylene oxide) copolymer surfactant as template. The WMS-39 has BET surface areas of 600–970 m^2/g and pore size around 3.9 nm. The polymer template is amphiphilic, which facilitates TEOS diffusing into the core of the template micelles. It is necessary to pre-hydrolyze TEOS prior to the condensation–polymerization directed by templates. The prehydrolysis time of TEOS has significant impact on the BET surface area, pore volume and yield. Thorough hydrolysis of TEOS favors large BET surface area, high pore volume and high yield. XRD and TEM results indicated that a 3-dimensional wormhole mesostructure was formed. Solid-state ^{29}Si MAS NMR suggested that calcinations facilitated further condensation reaction of the silanol groups in the silica matrix and simultaneously improve hydrophobicity of the samples. TGA/DTA analysis revealed three stages of weight loss of the as-synthesized WMS-39, which were primarily assigned to desorption of molecular water, decomposition and desorption of organic templates (100–500 °C), and water desorption, respectively. The assembly mechanism of the as-synthesized mesoporous silica was proposed.

Acknowledgements The authors are grateful to the AIF (Atlantic Innovation Foundation) Canada for financial support. The authors also express their thanks to Dr Michael Lumsden at the Dalhousie University for ^{29}Si MAS NMR analysis, and Dr Louise Weaver at the University of New Brunswick for TEM measurements.

References

1. Kresge CT, Leonowicz ME, Roth WJ, Vartuli JC, Beck JS (1992) Nature 359:710
2. Beck JS, Vartuli JC, Roth WJ et al (1992) J Am Chem Soc 114:10834
3. Turaga UT, Song C (2003) Catal Today 86:129
4. Klimova T, Calderon M, Ramirez J (2003) Appl Catal A: Gen 240:29
5. Liu BS, Xu DF, Chu JX, Liu W, Au CT (2007) Energy Fuels 21(1):250
6. Tanev PT, Pinnavaia TJ (1995) Science 267:865
7. Zhang W, Pauly TR, Pinnavaia TJ (1997) Chem Mater 9:2491
8. Zhang W, Frobea M, Pinnavaia TJ (1996) J Am Chem Soc 118:9164
9. Zhao D, Feng J, Huo Q, Melosh N, Fredrickson GH, Chmelka BF, Stucky GD (1998) Science 279:548
10. Zhao D, Huo Q, Feng J, Chmelka BF, Stucky GD (1998) J Am Chem Soc 120:6024
11. Stucky GD, Chmeka BF, Zhao D, Melosh N, Huo Q, Feng J, Yang P, Lukens W (1999) Int. Patent WO99/37705
12. Zhao D, Huo Q, Feng J, Kim J, Han Y, Stucky GD (1999) Chem Mater 11:2668
13. Huo Q, Feng J, Schueth F, Stucky GD (1997) Chem Mater 9:14
14. Huo Q, Leon R, Petroff PM, Stucky GD (1995) Science 268:1324
15. Huo Q, Margloese DI, Ciesia U, Feng P, Stucky GD (1994) Nature 367:317
16. Trong OD, Desplantier-Giscard D, Danumah C, Kaliaguine S (2001) Appl Catal A: Gen 222:299
17. Smarsly B, Polarz S, Antonietti M (2001) J Phys Chem B 105:10473
18. Flodstrom K, Alfredsson V (2003) Microporous Mesoporous Mater 59:167
19. Kipkemboi P, Fogden A, Flodstrom K (2001) Langmuir 17:5398

20. Hamley LW (2000) Introduction of soft matter. John Wiley & Sons, p 193
21. Coltan BK, Kelts LW (1994) In: Bergna HE (ed) The colloid chemistry of silica. American Chemical Society, pp 403–418
22. Pouxviel JC, Boilot JP (1987) J Non-Cryst Solids 89:345
23. Pavikovitch PI, Domhnail SCO, Neimark AV, Shuth F, Unger KK (1995) Langmuir 11:4765
24. Kruk M, Jaroniec M, Sayari A (1997) J Phys Chem B 101:583
25. Luken W, Schmidt-Winkel P, Zhao D, Feng J, Stucky GD (1999) Langmuir 15:5403
26. Trong OD, Kaliaguine S (2003) J Am Chem Soc 125:618
27. Kruk M, Jaroniec M, Ko C, Ryoo R (2000) Chem Mater 12:1961
28. Huo Q, Leon R, Petroff PM, Stucky GD (1995) Science 268:1324